SPARC-GE-04/002
09 September 2004

CONTRIBUTIONS TO FEL 2003

(8-12 September 2003, Tsukuba, Japan)

1) Status of the SPARC project

2) Evolution of transverse modes in a high-gain free-electron laser

3) A two-Frequency RF Photocathode Gun

4) Chirped pulse amplification at VISA-FEL

Available online at www.sciencedirect.com
SCIENCE DIRECT®
ELSEVIER
Nuclear Instruments and Methods in Physics Research A 528 (2004) 586–590
NUCLEAR INSTRUMENTS & METHODS IN PHYSICS RESEARCH Section A
www.elsevier.com/locate/nima

Status of the SPARC project

D. Alesini[a], S. Bertolucci[a], M.E. Biagini[a], C. Biscari[a], R. Boni[a], M. Boscolo[a], M. Castellano[a], A. Clozza[a], G. Di Pirro[a], A. Drago[a], A. Esposito[a], M. Ferrario[a], V. Fusco[a], A. Gallo[a], A. Ghigo[a], S. Guiducci[a], M. Incurvati[a], C. Ligi[a], F. Marcellini[a], M. Migliorati[a], C. Milardi[a], A. Mostacci[a], L. Palumbo[a], L. Pellegrino[a], M. Preger[a], P. Raimondi[a], R. Ricci[a], C. Sanelli[a], M. Serio[a], F. Sgamma[a], B. Spataro[a], A. Stecchi[a], A. Stella[a], F. Tazzioli[a], C. Vaccarezza[a], M. Vescovi[a], C. Vicario[a], M. Zobov[a], F. Alessandria[b], A. Bacci[b], I. Boscolo[b], F. Broggi[b], S. Cialdi[b], C. DeMartinis[b], D. Giove[b], C. Maroli[b], M. Mauri[b], V. Petrillo[b], M. Romè[b], L. Serafini[b,*], D. Levi[c], M. Mattioli[c], G. Medici[c], L. Catani[d], E. Chiadroni[d], S. Tazzari[d], R. Bartolini[e], F. Ciocci[e], G. Dattoli[e], A. Doria[e], F. Flora[e], G.P. Gallerano[e], L. Giannessi[e], E. Giovenale[e], G. Messina[e], L. Mezi[e], P.L. Ottaviani[e], S. Pagnutti[e], L. Picardi[e], M. Quattromini[e], A. Renieri[e], C. Ronsivalle[e], A. Cianchi[f], A.D. Angelo[f], R. Di Salvo[f], A. Fantini[f], D. Moricciani[f], C. Schaerf[f], J.B. Rosenzweig[g]

[a] *INFN-LNF, Via E.Fermi 40, 00044 Frascati (RM), Italy*
[b] *Università di Milano e INFN-Milano, Via Celoria 16, 20133 Milano, Italy*
[c] *INFN-Roma I, University of Roma "La Sapienza", p.le A. Moro 5, 00185 Roma, Italy*
[d] *INFN-Roma II, University of Roma "Tor Vergata", Via della Ricerca Scientifica 1, 00133 Roma, Italy*
[e] *ENEA-FIS, Via E. Fermi 45, 00040 Frascati (RM), Italy*
[f] *University of Roma "Tor Vergata", Via della Ricerca Scientifica 1, 00133 Roma, Italy*
[g] *UCLA—Department of Physics and Astronomy, 405 Hilgard Avenue, Los Angeles, CA 90024, USA*

Abstract

In this paper we report on the final design of the SPARC FEL experiment which is under construction at the Frascati INFN Laboratories by a collaboration between INFN, ENEA, ELETTRA, Un. of Rome (Tor Vergata), CNR and INFM. This project comprises an advanced 150 MeV photo-injector aimed at producing a high brightness electron beams to drive a SASE-FEL experiment in the visible using a segmented 12 m long undulator. The project, finally approved and funded early this year, has a 3 year time span, with the final goal of reaching saturation on the fundamental of the SASE-FEL and studying the resonant non-linear generation of harmonics. Peculiar features of this project are the optimized design of the photo-injector to reach minimum emittances by using flat-top laser pulses on the

*Corresponding author.
E-mail address: luca.serafini@mi.infn.it (L. Serafini).

0168-9002/$ - see front matter
doi:10.1016/j.nima.2004.04.107

photocathode, and the use of an uncompressed electron beam of 100 A peak current at very low emittance to drive the FEL. Results of start-to-end simulations carried out to optimize the performances of the whole system are presented, as well as the status of the construction and assembly of the system components. Activities planned for a second phase of the project are also mentioned: these are mainly focused on velocity bunching experiments that will be conducted with the aim to reach higher peak currents with preservation of low transverse emittances.

PACS: 41.60.Cr

Keywords: Photo-injector; High brightness electron beam; SASE-FEL; Non-linear resonant higher harmonics

1. Introduction

The overall SPARC Project consists of 4 main lines of activity. A *150 MeV Advanced Photo-Injector* aimed at investigating the generation of high brightness electron beams and their compression via magnetic and/or velocity bunching. This beam will be used to drive a *SASE-FEL Visible-VUV Experiment*: this is aimed to investigate the problems related to the beam matching into a segmented undulator and the alignment with the radiation beam at 500 nm, as well as the generation of non-linear coherent higher harmonics. In parallel, R&D activities are pursued at different sites on *X-ray Optics and Monochromators*, to analyze radiation-matter interactions in the spectral range of SASE X-ray FELs. Studies of *Soft X-ray table-top Sources* are also part of the SPARC program, with an anticipated upgrade of the present compact source at INFM-Politecnico Milano, delivering 10^7 soft X-ray photons in 10–20 fs pulses by means of high harmonic generation in a gas. In the following we present an overview of the system under construction at the Frascati National Laboratories of INFN, aiming at reaching the scientific and technological goals indicated in the first two topics listed above.

A 3D model of the whole system is illustrated in Fig. 1: the photo-injector, the FEL undulator, the beam dump and the undulator by-pass beam line are hosted inside a dedicated underground bunker which is 36 m long and 14 m wide.

The 150 MeV photo-injector consists of a 1.6 cell RF gun operated at S-band (2.856 GHz, of the BNL/UCLA/SLAC type) and high-peak field on the cathode (120 MV/m) with incorporated metallic photo-cathode (Cu or Mg), generating a 6 MeV beam [1]. The beam is then focused and matched into 3 SLAC-type accelerating sections, which boost its energy up to 150–200 MeV.The first section is embedded in solenoids in order to provide additional magnetic focusing to better control the beam envelope and the emittance oscillations [2]. The photo-cathode drive laser is a Ti:Sa system with the oscillator pulse train locked to the RF. To perform temporal flat top laser pulse shaping we will manipulate frequency lines in the large bandwidth of Ti:Sa, either using a liquid crystal mask in the Fourier plane for nondispersive optic arrangement or a collinear acousto-optic modulator [3] (DAZZLER). We aim achieving a pulse rise time shorter than 1 ps.

The photo-injector design is by now completed and is reported in a dedicated TDR [4] with full specification of each system component: all bids for acquisition of main components have been so far launched, so we expect to be on schedule with delivery of RF gun, laser system, RF sources and linac accelerating sections. The expected start of installation for the photo-injector components is

Fig. 1. A map view of the SPARC photo-injector and FEL undulator systems: from left to right, the RF gun, the first linac section embedded in solenoids, the two additional linac sections, the 6 undulator sections, the beam dump and the undulator by-pass beam line are visible.

confirmed for spring of 2005. The first beam at full energy is expected by the beginning of 2006.

2. Start-to-end simulations for the FEL experiment

A basic choice of SPARC phase 1 is to drive the FEL with an uncompressed beam: it was a decision by the project group to postpone the study of magnetic compression and velocity bunching to phase 2 of the project, as explained in Section 3. As a consequence, in order to make the FEL saturate with the natural beam current produced by the photo-injector one has to deliver at the undulator entrance a very high-quality (brightness) beam, i.e. with very low rms slice emittance and energy spread. To this aim we designed a photo-injector based on the Ferrario working point [2] lay-out to achieve full emittance compensation at the linac exit, where the emittance is no longer sensitive to envelope oscillations [5]. The selected beam parameters are listed in Table 1: they slightly differ from those of a previous analysis [6] because of the desire to keep a reasonable FEL saturation length with a bunch charge close to 1 nC. A peak current in excess of 100 A along a substantial fraction of the bunch is anticipated, despite the slight debunching caused in the gun to linac drift by the longitudinal space charge field. By properly matching the beam into the linac, set for on-crest acceleration at a gradient of 25 MV/m, the final rms normalized transverse emittance is minimized at the linac exit (155 MeV), with a nominal value of 0.75 μm as predicted by simulations: the corresponding slice emittance is about 0.6 μm over a substantial fraction of the bunch. A detailed analysis of errors and misalignments [4] in the system leads us to evaluate an upper limit for these two quantities as reported in Table 1, i.e. 2 μm for the rms normalized emittance and 1 μm for the slice emittance. The behavior of relevant beam parameters over the bunch slices is shown in Fig. 2: the energy spread is well below 0.06% for all slices and the current is above 100 A for 54% of the bunch slices. Matching this beam into the segmented undulator (parameters listed in Table 1) requires the use of two triplets in the transfer line in order to reduce the beta function of the beam down to about 1.5 m (average): to assure focusing in the horizontal plane along the undulator, single quadrupoles are located in undulator drift sections. Start-to-end simulations were performed using PARMELA [7] and GENESIS [8]: the result on FEL performances is shown in Fig. 3, where the FEL power growth along the undulator is plotted. Saturation power is reached at nearly 10^8 W in about 12 m of total length including drift sections, leaving some margin of extra undulator length. This comes out to be

Table 1
SPARC FEL experiment parameter list

Electron beam energy (MeV)	155
Bunch charge (nC)	1.1
Cathode peak field (MV/m)	120
Laser radius spot size on the cathode (mm, hard edge)	1.13
Laser pulse duration, flat top (ps)	10
Laser pulse rise time (ps) 10% → 90%	1
Bunch peak current at linac exit (A)	100
Rms norm. transv. Emittance at linac exit (μm); includes thermal comp. (0.3)	<2
Rms slice norm. emitt. (300 μm slice)	<1
Rms uncorrelated energy spread (%)	0.06
Undulator period (cm)	2.8
Undulator parameter, K	2.14
FEL radiation wavelength (nm)	499
Average beta function (m)	1.52
Expected saturation length (m)	<12

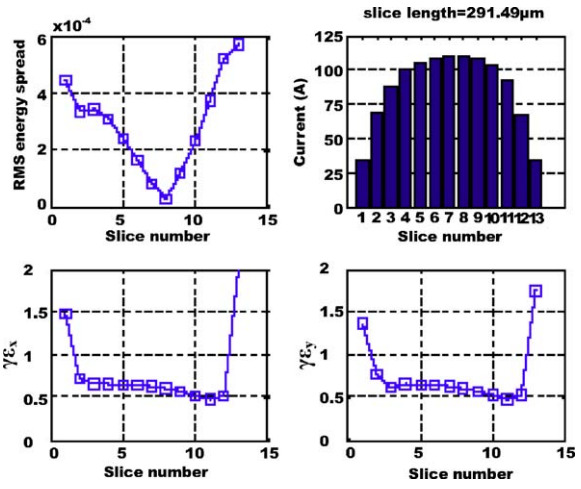

Fig. 2. Computed beam slice parameters at the photo-injector exit (energy spread, current, rms normalized emittance in x and y planes): the slice thickness is about 300 μm.

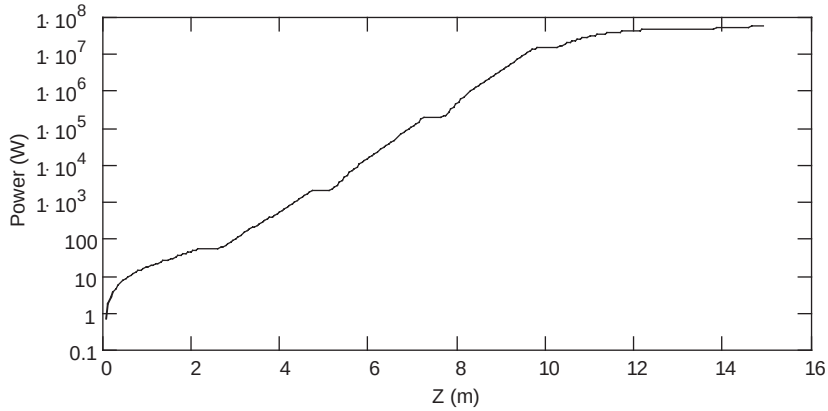

Fig. 3. FEL power growth simulated with GENESIS.

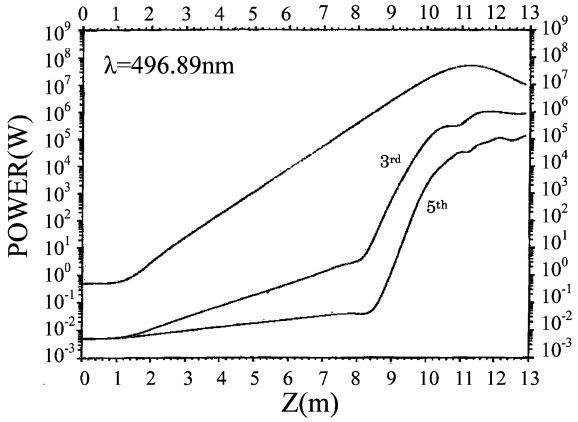

Fig. 4. FEL power growth on fundamental, third and fifth harmonic.

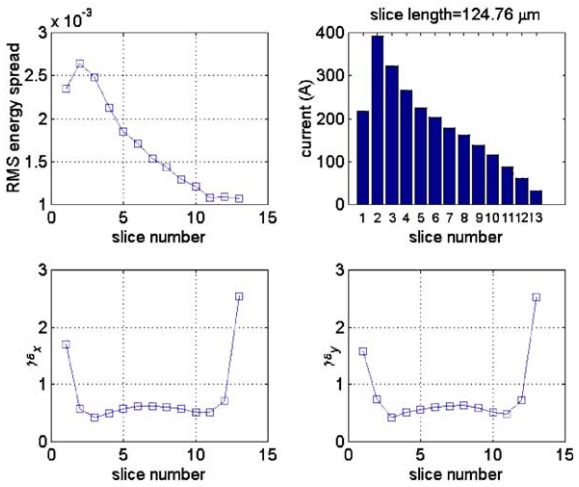

Fig. 5. Slice parameters at linac exit with weak velocity bunching.

important for the study of non-linear higher coherent harmonics: as a matter of fact, the power growth on the third and fifth harmonic, plotted in Fig. 4 as computed by the code PROMETEO [9], shows that saturation on these harmonics is reached some distance downstream that on the fundamental, hence requiring some additional undulator length. The saturation power level comes out to be nearly 2 and 3, respectively, orders of magnitude lower than the fundamental.

3. Phase 2 of the project

As previously mentioned, phase 1 of the SPARC Project was restricted to the use of uncompressed beams to drive the FEL experiment, mainly because of budget limitation issues. Full implementation of beam compression is foreseen in SPARC phase 2. As illustrated in Fig. 1, the second and third accelerating sections in the linac are not embedded in solenoids: in phase 2, expected to start in 2006, we plan to add solenoids to these sections in order to provide additional focusing along all the linac with flexible magnetic field profile. This is one of the most relevant demands of the velocity bunching technique [10]: it is needed to fully control envelope oscillations during compression, which in turns determine the

minimum emittance achieved. A magnetic compressor will also be installed on the second beam line to study CSR effects and emittance degradation issues. An example of possible performances that can be obtained by applying velocity bunching to the beam and by properly using the additional solenoid focusing provided in the last two sections, is shown in Fig. 5. By injecting the beam into the first section at -83°RF (0°RF corresponds to on-crest acceleration) at 25 MV/m, the beam current is raised up to 200 A for 40% of the bunch slices, with a slice at 400 A, while the slice emittance is kept below 0.6 μm for most slices (total rms normalized emittance is about 1.4 μm). We plan to perform a dedicated experimental investigation for characterizing the full potentiality of the velocity bunching technique.

References

[1] D.T. Palmer, The next generation photoinjector, Ph.D.Thesis, Stanford University.
[2] M. Ferrario, et al., Homdyn Study for the LCLS RF Photoinjector, SLAC-PUB 8400.
[3] F. Verluise, et al., Opt. Lett. 25 (2000) 572. See also S. Stagira, Proceedings of the Workshop on Laser Issues for Electron RF Photoinjectors, SLAC-WP-025, 2002.
[4] L. Palumbo, J.B. Rosenzweig (Eds.), Technical Design Report for the SPARC Advanced Photo-Injector, in publication.
[5] L. Serafini, J.B. Rosenzweig, Phys. Rev. E 55 (1997) 7565.
[6] D. Alesini, et al., Nucl. Instr. and Meth. A 507 (2003) 345.
[7] L.M. Young, J.H. Billen, Parmela, LA-UR-96–1835, 2000.
[8] S. Reiche, Nucl. Instr. and Meth. A 429 (1999) 243.
[9] G. Dattoli, et al., ENEA Report RT/INN/93/09 1993.
[10] L. Serafini, M. Ferrario, AIP Conf. Proc. 581 (2001) 87.

Available online at www.sciencedirect.com
SCIENCE DIRECT®
ELSEVIER
Nuclear Instruments and Methods in Physics Research A 528 (2004) 443–447
NUCLEAR INSTRUMENTS & METHODS IN PHYSICS RESEARCH Section A
www.elsevier.com/locate/nima

Evolution of transverse modes in a high-gain free-electron laser

S.G. Biedron[a,*], H.P. Freund[b], S.V. Milton[a,c], G. Dattoli[d], A. Renieri[d], P.L. Ottaviani[e]

[a] *MAX-Laboratory, University of Lund, Lund, Sweden SE-22100*
[b] *Science Applications International Corporation, McLean, VA 22102, USA*
[c] *Advanced Photon Source, Argonne National Laboratory, Argonne, IL 60439, USA*
[d] *ENEA, Unite Tecnico Scientifica Tecnologie Fisiche Applicate, Centro Ricerche Frascati, C.P. 65, 00044 Frascati, Rome, Italy*
[e] *ENEA, Divisione Fisica Applicata,Centro Ricerche E. Clementel, Via Don Fiammelli 2, Bologna, Italy*

Abstract

At the point of saturation in a high-gain free-electron laser (FEL) the light is fully transversely coherent. The number and evolution of the transverse modes is important for the effective tune-up and subsequent operation of FELs based on the photon beam characterization and in designing multi-module devices that rely on relatively stable saturation distances in each module. In the latter, this is particularly critical since each section will seed another module. Overall, in a single- or multi-module device, experimental users will desire stability in power and in photon beam quality. Using a numerical simulation code, the evolution of the transverse modes in the high-gain free-electron laser (FEL) is examined and is discussed. In addition, the transverse modes in the first few higher nonlinear harmonics are investigated.

PACS: 41.60; 42.65.Ky; 52.59.-f

Keywords: Free-Electron Lasers; Harmonic Generation; Frequency Conversion; Intense Particle Beams and Radiation Sources; Coherence

1. Introduction

A full understanding of the transverse coherence in a high-gain (HG), single-pass (SP), free-electron laser (FEL) as a function of distance is essential. If the gain process progresses differently than that designed, e.g. the FEL saturates before or after the end of the undulator, the transverse coherence properties will be affected. Knowledge of any such deviation from that expected is important for the user who requires knowledge of the coherence correlated to their data. A further challenge is the determination and control of the transverse coherence of the nonlinear harmonics, which do not necessarily saturate at the same longitudinal position as the fundamental and could also be more susceptible than the fundamental to the electron beam emittance and transverse electron beam distribution Nonlinear harmonics, see for example Ref. [1]. To predict the evolution of the transverse coherence of the fundamental and

*Corresponding author. Tel.: 46-46-222-3069; fax: 46-46-222-4710.
E-mail address: sgbiedron@elementaero.com (S.G. Biedron).

0168-9002/$ - see front matter © 2004 Elsevier B.V. All rights reserved.
doi:10.1016/j.nima.2004.04.128

nonlinear harmonics as a function of distance through a HG SP FEL, the simulation code MEDUSA [2] was modified to calculate and read out the intensity map for as many transverse modes as one requires to attain convergence of the transverse intensity profile. In this study, the development of the transverse intensity profile of two similar systems were studied: the SPARC project, managed by different Italian institutions [3] and the operational Low-Energy Undulator Test Line (LEUTL) at the Advanced Photon Source (APS) at Argonne National Laboratory (ANL) [4].

2. The simulation code—MEDUSA

MEDUSA is a 3D, multifrequency, macroparticle simulation code that represents the electromagnetic field as a superposition of Gauss–Hermite modes and uses a source-dependent expansion to determine the evolution of the optical mode radius. The field equations are integrated simultaneously with the 3D Lorentz force equations. MEDUSA differs from the other nonlinear simulation codes in that no undulator-period average is imposed on the electron dynamics. It is capable of treating quadrupole and corrector fields, magnet errors, and multiple segment undulators of various quantities and types. MEDUSA is able to treat the fundamental and all harmonics simultaneously. Because of these features, MEDUSA is capable of following the FEL evolution of the fundamental and all harmonics. Most recently, diagnostic output of the mode pattern as a function of axial position has been added to MEDUSA.

3. Cases under study

Using MEDUSA, the fundamental and nonlinear harmonics were simulated to investigate the evolution of the transverse modes and intensity profile in the theoretical cases of the SPARC project in Italy and the LEUTL at the APS at ANL. The parameters for the SPARC project are from an earlier iteration of the present design parameters. These SPARC and LEUTL parameters are listed in Table 1.

Table 1
Parameters of the SPARC Project in Italy and those of LEUTL at the APS ANL

Parameters	SPARC	LEUTL
Electron beam energy (MeV)	150	219.5
Normalized emittance (π mm-mrad)	2	5
Peak current (A)	150	150
Undulator period (m)	0.033	0.033
Undulator strength (K)	1.886	3.1
Energy spread (%)	0.1	0.1
Fundamental wavelength (nm)	529.6	518.8

4. Results

In both cases, the fundamental and the third and fifth harmonics were simulated and the mode structure was mapped out after each undulator segment in the conceptual design of the SPARC system and in the actual LEUTL system. A flat-pole-face wiggler model was used with quadrupole focusing between each undulator section. The fundamental was seeded with 10 W of optical power and the harmonics were started at zero power. Note that since the fundamental was seeded with 10 W of optical power, we ran MEDUSA in the amplifier mode of operation. The difference between SASE and amplifier operation in FELs is largely (1) the start-up from noise region, and (2) the spectral bandwidth. Once the start-up regime is passed, however, the fields grow exponentially as in an amplifier. Further, once saturation is reached in a SASE FEL, the spectral narrows about the wavelength of the fastest-growing mode. Hence, an amplifier model can give a reasonable simulation of a SASE FEL as long as the fastest-growing mode is used along with a good estimate of the start-up noise power. The self-amplified spontaneous emission (SASE) case, or start up from noise case, now requires investigation. Twenty five modes were used with a total of 34,992 particles.

4.1. SPARC

In the SPARC case, the powers of the fundamental, third harmonic, and fifth harmonic are

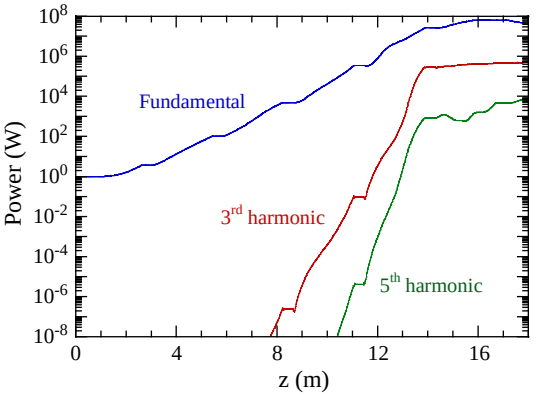

Fig. 1. Fundamental, 3rd harmonic, and 5th harmonic FEL power (W) growth as a function of distance, z (m), through the SPARC undulator system.

plotted in Fig. 1 as a function of distance through the HG SP FEL. Note the points of saturation vary for the wavelength (or harmonic), as evidenced in Fig. 1 as well as in Figs. 2 and 3 in greater detail. In these latter figures, the horizontal (x) and vertical (y) intensity cross the sections for $y = 0$ and $x = 0$, respectively, as a function of distance for the fundamental, third harmonic, and fifth harmonic are shown. The cross-sections are those following each undulator section (every 70 periods), the points at which MEDUSA was programmed to write out the extensive modal information. All cross-sections have been normalized to a peak intensity of 1 and offset in both x and y to allow easier viewing of the propagation along the length of the undulator. The fundamental saturation occurs between the 4th and 5th undulators, the third harmonic saturation occurs between the 5th and 6th undulators, and the fifth harmonic saturation occurs between the 6th and 7th undulators. To determine the exact positions of saturation of each wavelength, an extensive numerical undertaking is required with the code to read out many more modal maps in z. At the points of near saturation, the narrowing of the modes is clear and the mode narrowing increases as a function of harmonic number. Note that the maximum output power does not necessarily provide the "cleanest" mode structure—closest to TEM_{00}—for the FEL user, when comparing Fig. 1 with Figs. 2 and 3. In other words—it is insufficient to only examine the output

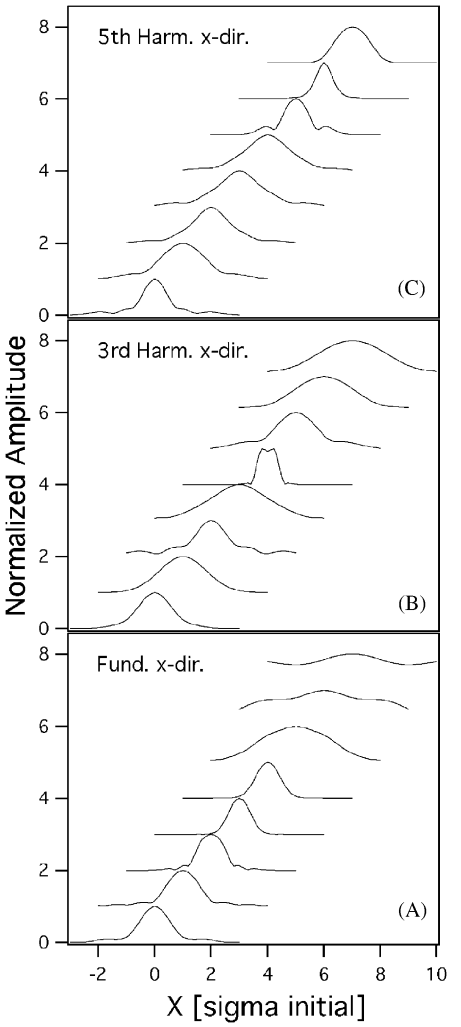

Fig. 2. Intensity profile cross-sections in the x-direction (wiggle plane) for $y = 0$. The lower left is following the first undulator and the profiles toward the 8th undulator is offset up and to the right for clarity. (A) Fundamental wavelength (532.1 nm), (B) 3rd harmonic (177.4 nm), and (3) 5th harmonic (106.4 nm).

power as a function of distance in planning for future user facilities that intend to employ non-linear harmonic FEL radiation—the beam physicist must *also* examine the mode structure of each wavelength. Please also note that when designing and optimizing an FEL, a much higher resolution of the transverse mode development for the fundamental and harmonics must be simulated. In this paper, however, we intend only to outline the importance of investigating the evolution of

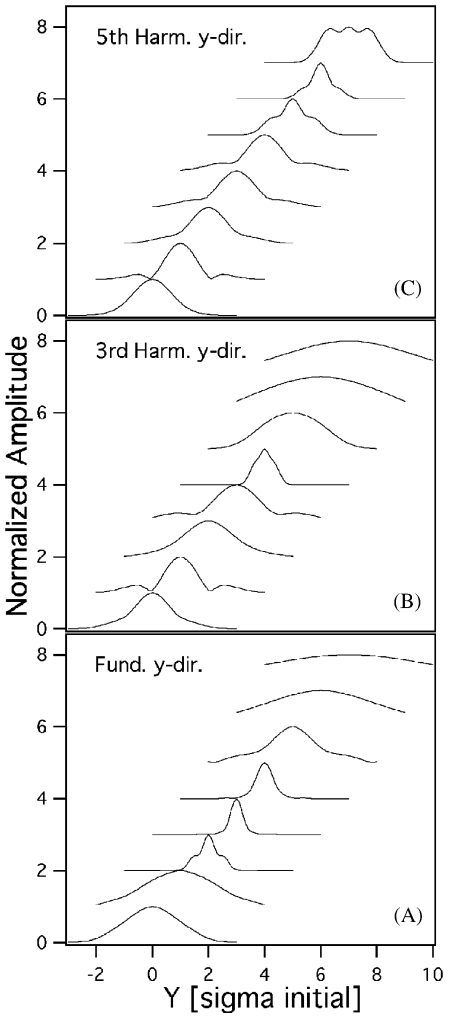

Fig. 3. Intensity profile cross-sections in the y-direction (opposite to the wiggle plane) for $x=0$. The lower left is following the first undulator and the profiles toward the 8th undulator is offset up and to the right for clarity. (A) Fundamental wavelength (532.1 nm), (B) 3rd harmonic (177.4 nm), and (C) 5th harmonic (106.4 nm).

the fundamental and harmonics for the design of future user facilities.

Saturation of the fundamental occurs near the end of the 5th undulator. In both the x and y directions the cross-sections tend toward a true TEM_{00} mode as the intensity grows toward saturation and beyond. At saturation, this mode size begins to grow since the so-called gain guiding is no longer effective. Also following saturation, additional modes tend to gain on the TEM_{00} mode and the intensity profile loses its strictly Gaussian shape.

The intensity profile of the harmonics behave differently due to the shorter gain length. There seems to be no true mode that the profile settles down to. There are differences in x and y. These nonlinear harmonics are very much a product of the fundamental interaction and are entirely dependent upon it. Furthermore, although the beam emittance is below the diffraction limit in the case of the fundamental this is not necessarily the case for the harmonics. The 5th harmonic, for example, does not meet the diffraction limit criteria of $\varepsilon<\lambda/4\pi$. The harmonics can be therefore, much more susceptible to the actual electron beam distribution.

4.2. LEUTL

Similar results were obtained for the LEUTL case. The fundamental transverse intensity distribution tends toward a true TEM_{00} mode at saturation, Fig. 4, and begins to deviate from this beyond saturation. The harmonics, as in the case of the SPARC, have a very rich mode content as shown in Fig. 5; the third harmonic beyond the saturation point in the LEUTL case.

5. Conclusions

We have added diagnostics to the MEDUSA simulation code in order to explicitly study the evolution of the transverse amplitude profile in a future light source, and have applied the code to study this evolution in the SPARC and LEUTL projects. This approach can be used to determine the profile evolution and transverse coherence in future light sources. The transverse mode evolution of the fundamental and harmonics vary with longitudinal position and differ based upon specific electron beam and undulator properties. In the case of an operational facility, the transverse coherence and intensity profile at the exit of the undulator line will be important for some of the user experiments. Small variations in electron beam quality may lead to unwanted variations shot-to-shot. This is particularly true for the

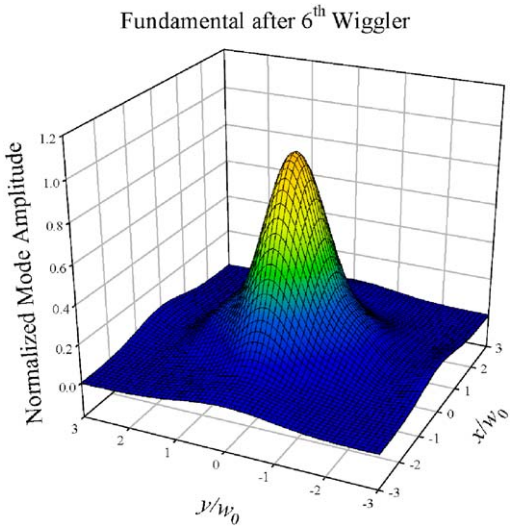

Fig. 4. LEUTL fundamental signal after saturation.

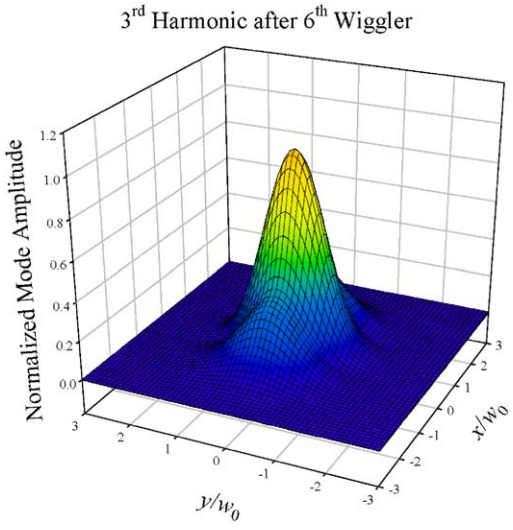

Fig. 5. LEUTL third harmonic signal near saturation.

harmonics and even partly true for the fundamental beyond saturation. These effects may be more pronounced as the wavelengths get shorter and the electron beam emittance approaches or exceeds the optical mode emittance such as in an X-ray SASE source.

The next step in the investigation of the transverse modes is to examine a system more thoroughly by analyzing the evolution at numerous more longitudinal positions, with start-up from noise to simulate SASE operation, and to simulate the far-field behaviour of the radiation. These three extensions will greatly benefit the future FEL users. It is hoped that a comparison can be made with experiment in the near future after these additional goals are achieved.

Acknowledgements

The activity and computational work for H. P. Freund is supported by Science Applications International Corporation's Advanced Technology Group under IR&D subproject 01-0060-73-0890-000. The work of S.V. Milton is supported at Argonne National Laboratory by the US Department of Energy, Office of Basic Energy Sciences under Contract No. W-31-109-ENG-38. The work of G. Dattoli, P.L. Ottaviani, and A. Renieri is supported by ENEA the Italian Agency for New Technologies, Energy, and the Environment.

We wish to thank our colleagues and collaborators for encouraging us to pursue these transverse mode efforts, albeit in our spare time: B. Faatz, R. Bartolini, S. Benson, F. Ciocci, R. Dejus, W.M. Fawley, G. Felici, L. Gianessi, Z. Huang, K-.J. Kim, J. Lewellen, Y. Li, A. Lumpkin, G. Neil, and J. Rocca.

References

[1] S.G. Biedron, Z. Huang, K.-J. Kim, S.V. Milton, G. Dattoli, A. Renieri, W.M. Fawley, H.P. Freund, H.-D. Nuhn, P.L. Ottaviani, Phys. Rev. St. Accel. Beams 5 (2002) 030701 and references therein.

[2] H.P. Freund, T.M. Antonsen Jr.,, Principles of Free-electron Lasers, 2nd Edition, Chapman & Hall, London, 1986;
H.P. Freund, Phys. Rev. E 52 (1995) 5401;
S.G. Biedron, H.P. Freund, S.V. Milton, Development of a 3D FEL code for the simulation of a high-gain harmonic generation experiment, in: H.E. Bennett, D.H. Dowell (Eds.), Free Electron Laser Challenges II, Proceedings of SPIE, Vol. 3614, 1999, p. 96;
H.P. Fruend, et al., IEEE J. Quant. Electron. 36 (2000) 275.

[3] A. Renieri, Nucl. Instr. and Meth. A 507 (2003) 507.

[4] S.V. Milton, et al., Science. 292 (5524) (2001) 2037. (Originally published in Science Express as 10.1126/science. 1059955 on May 17, 2001).

Available online at www.sciencedirect.com
SCIENCE DIRECT®
ELSEVIER
Nuclear Instruments and Methods in Physics Research A 528 (2004) 316–320
NUCLEAR INSTRUMENTS & METHODS IN PHYSICS RESEARCH Section A
www.elsevier.com/locate/nima

A two-Frequency RF Photocathode Gun

D.H. Dowell[a,*], M. Ferrario[b], T. Kimura[c], J. Lewellen[d], C. Limborg[a], P. Raimondi[b], J.F. Schmerge[a], L. Serafini[e], T. Smith[c], L. Young[f]

[a] *Stanford Linear Accelerator Center, Mail Stop 18, 2575 San Hill Rd., Menlo Park, CA 94025-7015, USA*
[b] *INFN-Frascati, via E. Fermi 40, 00040 Frascati, Italy*
[c] *Hansen Labs, Stanford University, Stanford, CA 94305-4085, USA*
[d] *Advanced photron Source, Argonne National Laboratory, Argonne, IL 60439, USA*
[e] *INFN-Milan-LASA, via Fratelliceni 201, 20090 Segrate (MI), Italy*
[f] *Los Alamos National Laboratory, P.O. Box 1663, Los Alamos, NM 87545, USA*

Abstract

In this paper we resurrect an idea originally proposed by Serafini (Nucl. Instr. and Meth. A 318 (1992) 301) in 1992 for an RF photocathode gun capable of operating simultaneously at the fundamental frequency and a higher frequency harmonic. Driving the gun at two frequencies with the proper field ratio and relative phase produces a beam with essentially no RF emittance and a linear longitudinal phase space distribution. Such a gun allows a completely new range of operating parameters for controlling space charge emittance growth. In addition, the linear longitudinal phase space distribution aids in bunch compression. This paper will compare results of simulations for the two-frequency gun with the standard RF gun and the unique properties of the two-frequency gun will be discussed.

PACS: 29.25.Bx; 29.27.Ac; 41.60.Cr; 41.85.Ar

Keywords: Electron beam; Photocathode RF gun; RF harmonics; Emittance

1. Introduction

The RF gun transverse emittance is predominately due to space charge forces, RF fields and thermal emittance. Emittance compensation does well to remove the linear space charge contribution, but the gun parameters are still constrained to operate between the space charge and RF limits. This is illustrated in Fig. 1, where the uncompensated emittance at the gun exit is plotted in the plane defined by beam size and bunch length. The operating region is shown for the LCLS gun and is typical of most guns. They perform best in the saddle between the space charge and RF dominated regimes. Emittance compensation extends the region into the space charge regime, and does a remarkably good job of recovering the emittance where the correct combination of solenoid, drift and linac gradient and phase, reduce the projected emittance from three microns to one micron after

*Corresponding author. Tel.: +1-650-9262494; fax: +1-650-926-8533.
E-mail address: dowell@slac.stanford.edu (D.H. Dowell).

0168-9002/$ - see front matter © 2004 Elsevier B.V. All rights reserved.
doi:10.1016/j.nima.2004.04.078

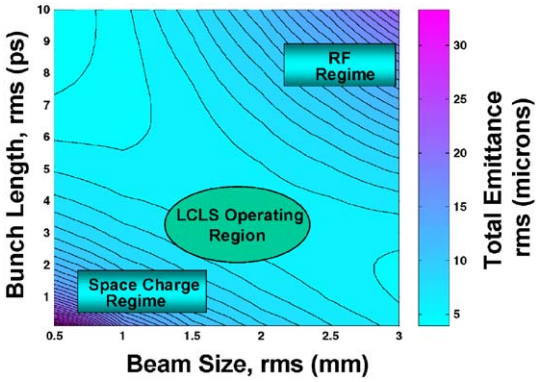

Fig. 1. Contour plot of the total emittance at the gun exit in the plane of bunch size and length. The bunch charge is 1 nC. The formulas of Travier [1] were used to compute the RF and space charge effects.

acceleration to high energy. However, further improvement requires one to advance from compensating to eliminating the sources of the emittance.

It has been shown [2] that the addition of a harmonic to the RF fundamental field would greatly reduce the RF emittance, allowing complete freedom of beam size and length to control the space charge forces. This work showed a harmonic RF field in the same $N+\frac{1}{2}$ cells as the fundamental will linearize the RF force to fourth order, both transversely and longitudinally. This condition is achieved when the bunch exit phase is $\pi/2$, $n = 3,7,11\ldots$ and the nth harmonic field, E_n, in terms of the fundamental field, E_0, is given by

$$E_n = (-1)^{(n-3)/2} E_0/n^2.$$

This work resurrects these ideas and applies them to the BNL/SLAC/UCLA gun. The space charge and RF-dominated regimes are simulated with a new version of Parmela [3] capable of superimposing the RF fields at two frequencies in the same cell. Short bunches are used to explore the space charge dominated regime while long bunches investigate the RF-dominated regime. In addition, the two-frequency gun is combined with emittance compensation to achieve very low transverse emittance. Comparisons of the transverse and longitudinal emittances and phase space distributions are presented and discussed.

2. Superfish fields

The standard 1.6 cell BNL/SLAC/UCLA shape was modified to have the desired fundamental and 3rd harmonic frequencies while keeping the 1.6 $\lambda/2$ length. The field shapes for the Superfish model are shown in Fig. 2. The gun's fundamental mode is unbalanced due to the shape change used to obtain the harmonic. The cathode cell 3rd harmonic is a TM021-like mode and the full cell mode is TM012-like, which should not significantly affect our results since the beam samples only the on-axis fields.

3. The parmela simulations

The simulations were designed to explore the two-frequency gun's properties in both the space charge and RF regimes. The study compares emittances for short, space charge dominated bunches with emittances for long, RF-dominated bunches. The longitudinal electric field is assumed to be the sum of the fundamental and the 3rd harmonic fields given by

$$E_z = E_0 \cos(kz)\sin(\omega t + \phi_0) + E_3 \cos(3kz)\sin(3(\omega t + \phi_3)).$$

In each case, the parameters ϕ_0, E_3 and ϕ_3 are varied to obtain the lowest projected emittance.

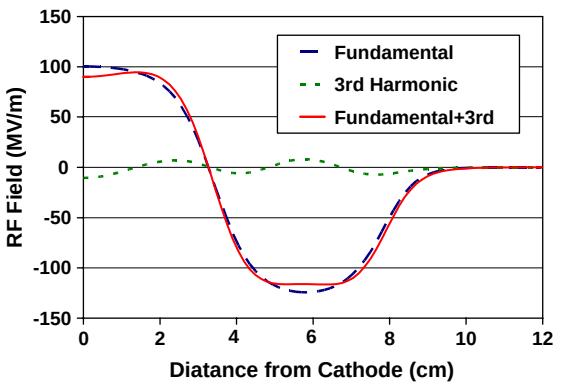

Fig. 2. The Superfish fields used in the Parmela simulations. The full cell field is approximately 20% higher than the cathode cell field.

For both the short and long bunch simulations, the beam size on the cathode is 2 mm radius, flat top distribution and the results are given at the gun exit, with no solenoid field or any emittance compensation. The space charge regime (short bunch) uses a 10 ps full-width, square bunch shape. The RF regime (long bunch) is studied with a 40 ps long bunch. Simulations are performed with 0 and 1 nC to separate the RF and space charge contributions.

For the emittance compensated case the beam radius is 1 mm and the full-width bunch length is 30 ps. In all cases, the thermal emittance is zero.

3.1. Longitudinal phase space

Fig. 3 shows that even for short bunches 3rd harmonic linearization improves the longitudinal phase space. The full-width, correlated energy spread is reduced from 100 to 40 keV in the presence of space charge.

The short bunch case for 0 nC, RF only, is shown in Fig. 4. The addition of the 3rd harmonic not only makes the distribution more linear, but also flips the sign of the correlation. This is not observed in the analytic theory [2], and is due to the 1.6 cell length of the gun used in these simulations. The original theory is for a 1.5 cell gun. In addition, the figure shows the fundamental phase which produces the lowest transverse emittance is slightly different than that which best linearizes the longitudinal phase space.

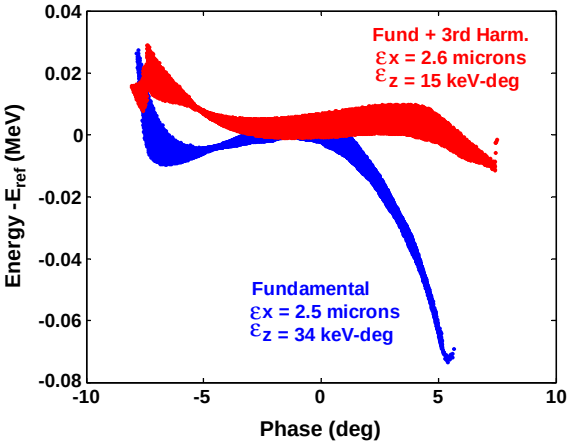

Fig. 3. The short bunch longitudinal phase space at 1 nC with and without the 3rd harmonic: $E_0 = 82$ MV/m, $\phi_0 = 25°$, $E_3 = -21$ MV/m, $\phi_3 = 17°$.

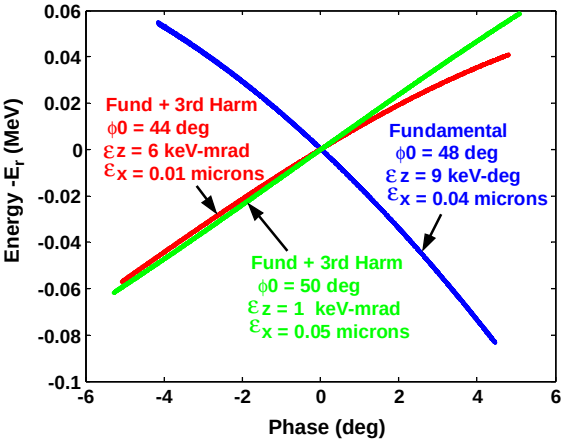

Fig. 4. Longitudinal phase space with 0 nC of charge, 10 ps full-width for fundamental only and fundamental + 3rd harmonic: $E_0 = 82$ MV/m, $E_3 = -28$ MV/m, $\phi_3 = 15°$, ϕ_0 as shown.

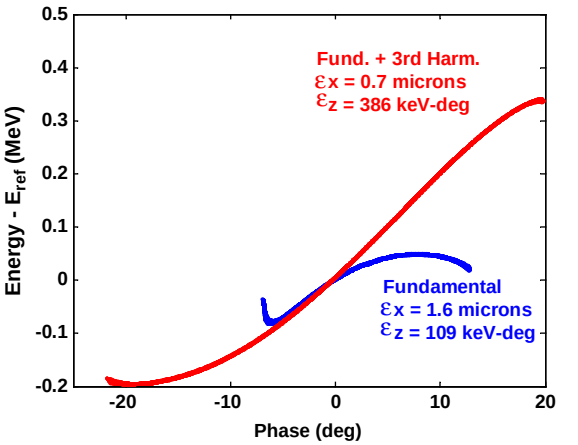

Fig. 5. The 40 ps long bunch longitudinal phase space at 1 nC with and without the 3rd harmonic. For fundamental only: $E_0 = 82$ MV/m, $\phi_0 = 20°$. For fundamental + harmonic: $E_0 = 82$ MV/m, $\phi_0 = 35°$, $E_3 = -31.5$ MV/m, $\phi_3 = 17°$.

The 40 ps long bunch for a 1 nC bunch is shown in Fig. 5. With only the fundamental, the bunch has been compressed approximately by a factor of two. However, with the 3rd harmonic, the bunch length is unchanged.

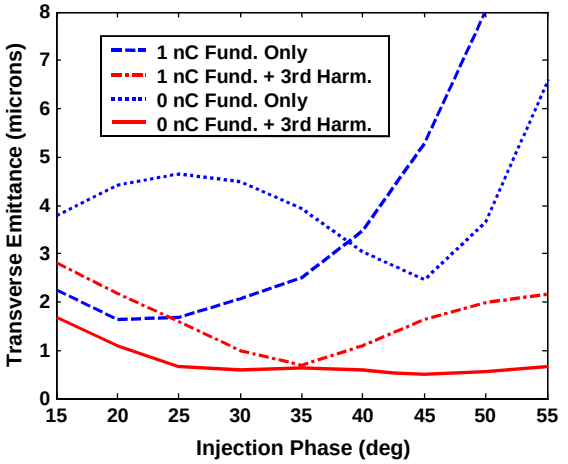

Fig. 6. Transverse projected emittance for a 40 ps long square bunch. For 0nC: $E_0 = 82\,\mathrm{MV/m}$, $\phi_0 = 35^\circ$, $E_3 = -28\,\mathrm{MV/m}$, $\phi_3 = 16^\circ$. For 1 nC: $E_0 = 82\,\mathrm{MV/m}$, $\phi_0 = 35^\circ$, $E_3 = -31.5\,\mathrm{MV/m}$, $\phi_3 = 18^\circ$. Although the minimum projected emittance is larger for 0 nC at 45° injection phase than for 1 nC at 25°, the 0°nC slice emittance is smaller over more of the bunch. Slice mismatch makes the 0°nC emittance larger than 1 nC emittance.

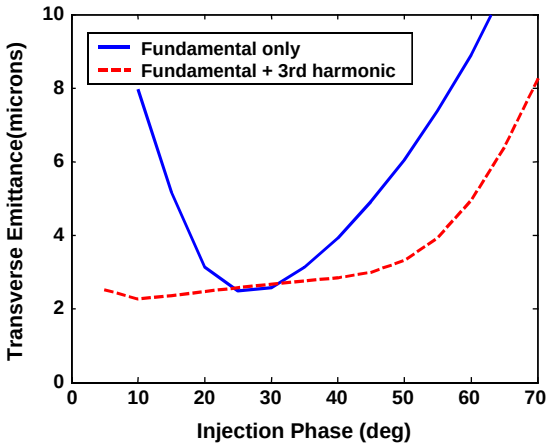

Fig. 7. Short bunch transverse emittance for 1 nC at the exit of RF gun without and with the 3rd harmonic field: $E_0 = 82\,\mathrm{MV/m}$, $\phi_0 = 25^\circ$, $E_3 = -21\,\mathrm{MV/m}$, $\phi_3 = 17^\circ$.

3.2. Transverse emittance

It is expected that the 3rd harmonic should mostly benefit long bunches in the RF dominant regime. In this case, the RF emittance is expected to be small over a wide range of injection phases as given in the original work [2]. Fig. 6 shows this is verified by the Parmela simulations, reducing the RF emittance a factor of four or more for injection phases from 25° to 55°. With the addition of space charge, the fundamental + 3rd harmonic emittance is approximately half that of the fundamental only value.

The results of both frequencies upon the emittance for a short, space charge dominated bunch is given in Fig. 7. While the fundamental + 3rd minimum projected emittance is not any lower than that with the fundamental alone, the

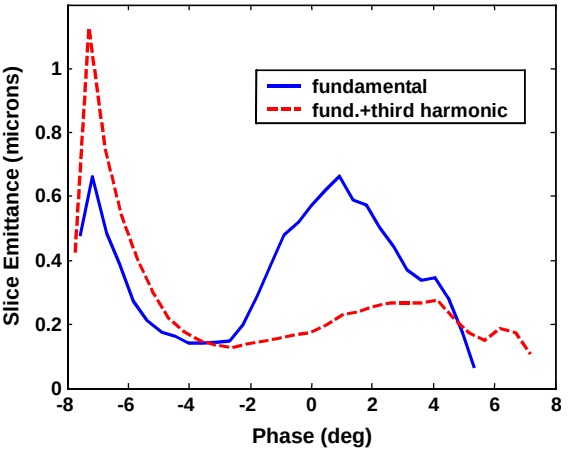

Fig. 8. The short-bunch, slice emittance for 1 nC is plotted as a function of position along the bunch. The head of the bunch is to the left and 1° at s-band = 1.05 ps. $E_0 = 82\,\mathrm{MV/m}$, $\phi_0 = 35^\circ$, $E_3 = -21\,\mathrm{MV/m}$, $\phi_3 = 17^\circ$.

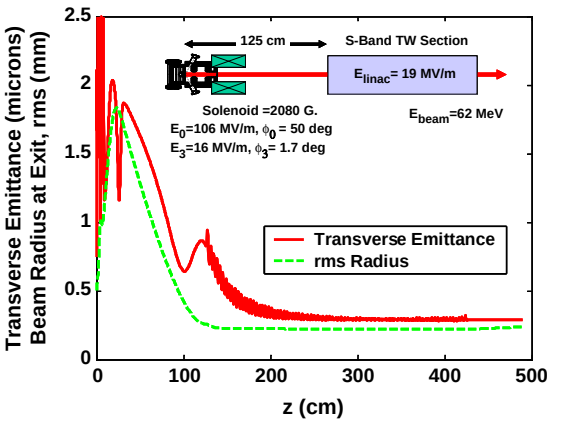

Fig. 9. The projected transverse emittance and beam size of the two-frequency gun with emittance compensation. The final bunch length is 29 ps full-width.

beam quality is good over a wider range of injection phase, even indicating some improvement down to 10°.

The reduction in the short bunch slice emittance is larger. Fig. 8 gives the slice emittance plotted along the length of the bunch in degrees of RF and indicates that except for the head slices, the emittances are reduced from 0.6 to 0.3 μm or less over the main body of the bunch.

The configuration and simulation results for the emittance compensation case are shown in Fig. 9 for a 30 ps long, 1 nC bunch. The projected emittance equilibrates to 0.28 μm and the slices (not shown) are very well aligned with emittances of 0.2 μm over more than 95% of the bunch.

Acknowledgements

SLAC is operated by Stanford University for the Department of Energy under contract number DE-AC03-76SF00515.

References

[1] C. Travier, Nucl. Instr and Meth. A 340 (1994) 26.
[2] L. Serafini et al, Nucl. Instr and Meth. A 318 (1992) 301; T.I. Smith, Proceedigs of the Linear Account Conference, SLAC PUB-303.
[3] L.M. Young, "PARMELA," Los Alamos National Laboratory Report LA-UR-96-1835(revised July17, 2003).

Available online at www.sciencedirect.com
SCIENCE DIRECT®
ELSEVIER
Nuclear Instruments and Methods in Physics Research A 528 (2004) 463–466
NUCLEAR INSTRUMENTS & METHODS IN PHYSICS RESEARCH Section A
www.elsevier.com/locate/nima

Chirped pulse amplification at VISA-FEL

R. Agustsson[a], G. Andonian[a], M. Babzien[b], I. Ben-Zvi[b], P. Frigola[a], J. Huang[c], A. Murokh[a,*], L. Palumbo[d], C. Pellegrini[a], S. Reiche[a], J. Rosenzweig[a], G. Travish[a], C. Vicario[d], V. Yakimenko[b]

[a] *Department of Physics Astronomy, University of California, 405 Hilgard Ave., Los Angeles, CA 90095-1547, USA*
[b] *Brookhaven National Laboratory, Upton, NY 11973, USA*
[c] *Phoang Accelerator Laboratory, South Korea*
[d] *University of Rome, "La Sapienza", Italy*

Abstract

Chirped beam manipulations are of the great interest to the free electron laser (FEL) community as potential means of obtaining ultra short X-ray pulses. The experiment is under way at the accelerator test facility (ATF) at Brookhaven National Laboratory (BNL) to study the FEL process limits with the under-compressed chirped electron beam. High gain near-saturation SASE operation was achieved with the strongly chirped beam (~2.8% head-to-tail). The measured beam dynamics and SASE properties are presented, as well as the design parameters for the next round of experiment utilizing the newly installed UCLA/ATF chicane compressor.

PACS: 41.60.Cr

Keywords: Short pulse; SASE FEL

1. Introduction

With the prospects of the X-ray free electron laser (FEL) becoming a reality within the next decade [1], there is a great interest in a broader scientific community towards shortening the pulse duration of the anticipated X-ray FEL pulses down to 10-femtosecond range. For example, it would allow singular molecule diffraction experiments in the time interval shorter than it takes for the Coulomb explosion to destroy the sampled molecule [2]. Recently it was proposed [3] to use a chirped electron bunch to drive the self-amplified spontaneous emission (SASE) FEL so that the resulted SASE frequency modulation could allow separating single lasing spike from the rest of the bunch, or even using the optical gratings to longitudinally compress the X-ray beam. The limits associated with the chirped electron beam based SASE process have been studied theoretically and through simulations [4,5], and one can

*Corresponding author.
E-mail address: murokh@physics.ucla.edu (A. Murokh).

0168-9002/$ - see front matter © 2004 Elsevier B.V. All rights reserved.
doi:10.1016/j.nima.2004.04.132

approximately state, that the characteristic chirp value of interest is given by

$$\left(\frac{\Delta p}{p}\right)\frac{\lambda_c}{L_b}\sim\rho \quad (1)$$

where λ_c and L_b are the FEL cooperation length [6] and the electron beam bunch length respectively, and ρ is the 3-D FEL parameter. The amount of electron beam chirp indicated in Eq. (1) is sufficient to separate individual spikes in time and frequency domain, while still preserving high gain SASE operation (which gain length generally increases with the higher uncorrelated energy spread).

2. Description of the VISA experimental system

The experiment is under way at VISA-FEL (visible to infrared SASE amplifier) to demonstrate a proof of principle, that the efficient chirped SASE amplification is possible with the electron beam chirp value of interest as is indicated in Eq. (1). The experiment is driven by the high brightness ATF photoinjector beam of about 71 MeV, matched into the strong focusing VISA undulator ($\beta_x,\beta_y\sim 30$ cm). The original VISA-I experiment in 2001 demonstrated SASE high gain and saturation within 4-m undulator at 840 nm [7,8].

To achieve high gain SASE lasing, an unusual bunch compression mechanism is used, utilizing nonlinear properties of the long dispersive section in the ATF beam line (Fig. 1); which is taking advantage of the large negative second order compression coefficient T_{566}. The initial electron bunch (Table 1) with the current of 55 A is

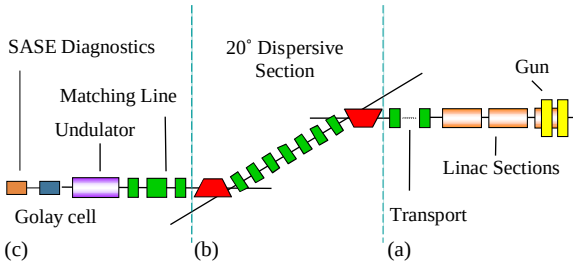

Fig. 1. Experimental layout of the ATF Beam line III: gun and linac area (a); 20° double-bend dispersive section (b); and VISA experimental area (c), including the undulator and diagnostics.

Table 1
Electron beam characteristics and FEL gain length measured without compression (A) and with compression (B)

	Case A	Case B
Electron beam energy	71.2 MeV	70.4 MeV
Beam charge, Q	300 pC	300 pC
Horizontal emittance, ε_n	2.1 ± 0.2 μm	~4 μm
Peak current, I_p	55 A	~300 A
Sliced energy spread, $\Delta\sigma_\gamma$	0.05%	0.45%
FEL gain length, L_g	~30 cm	~20 cm

compressed longitudinally up to the peak current of 300 A, through manipulating the beam line tune settings, electron beam RMS linear chirp, σ_γ, and central momentum offset of the electron bunch, $\Delta p/p$:

$$\Delta\zeta=\left(T_{566}\frac{\Delta p}{p}\right)\sigma_\gamma. \quad (2)$$

The typical chirp value to obtain maximum compression was of the order of $\sigma_\gamma\sim0.17\%$, during VISA-I experiment. Even though such a compression process allowed obtaining short FEL gain length and corresponding studies of the SASE properties at saturation, it had significantly restricted controllability of the electron beam parameters.

On the other hand, in accordance with the Eq. (1), an electron beam chirp of about 2% is required to demonstrate chirped beam amplification of interest, which is an order of magnitude larger value than used during VISA-I. The new ongoing round of experiments (VISA-II) [9] has two stages: (1) initial optimization of the beam line tune and beam running conditions to achieve SASE operation with the large chirp (Table 1B); and (2) the main part involving utilization of the magnetic chicane compressor at ATF and electron beam transport linearization to achieve independent control over the electron beam chirp and longitudinal bunch profile.

3. Initial experimental results on the chirped beam amplification

One of the challenges of running a strongly chirped electron beam through the ATF beam line

is to control the size of the beam, through the dispersion section of the beam line. The chirped beam transmission through the beam line is controlled by the high-energy slit (HES), which is an adjustable collimator located at the beginning of the dispersive section. In the recent experimental round, the 500 pC electron beam (Fig. 1a) has a 2.8% energy chirp after the linac exit, of which only 1.7% (330 pC) can propagate through the fully open HES (Fig. 2b).

The compression process in the dispersive section is monitored by the Golay cell installed in front of the undulator to measure the coherent transition radiation (CTR) intensity [8]. When the beam central momentum is chosen to optimize the compression in the dogleg, the CTR energy is peaked. Then, by closing the HES one can determine the part of the beam that contributes to the compression process (Fig. 2c). The start-to-end PARMELA-ELEGANT simulations reproduced the compression process as observed by the combined slit and Golay cell measurements showing that the bunch peak current enhancement can reach up to 300 A.

With such a current very high SASE gain is achieved, despite the large sliced energy spread and degraded sliced emittance in the compressed part of the beam. The average SASE radiated energy around 2 μJ was recorded, which is within the order of magnitude from the saturation level. The spectrum of the FEL radiation (Fig. 3) have unusual width of up to 10%, and a characteristic dual spike structure, indicating two lasing modes. It should be noted, that by closing the HES, one could eliminate one of the spectral spikes, without degrading the second spike intensity (Fig. 2d), indicating longitudinal mapping of the SASE wavelength to the electron beam chirp. Yet, the detailed GENESIS simulations, and further measurements are necessary to confidently reproduce the SASE process under these non-trivial experimental conditions.

Another interesting observation is the unusual stability of the SASE process. Because the beam chirp is very linear and only 60% propagates through the HES, the FEL performance becomes insensitive to the RF phase jitter. Unlike in VISA-1, where small drifts in the RF phase would degrade lasing significantly, in this new, large chirp regime, the same beam fraction propagates through HES, regardless of the beam centroid jitter, thus making the lasing much more stable.

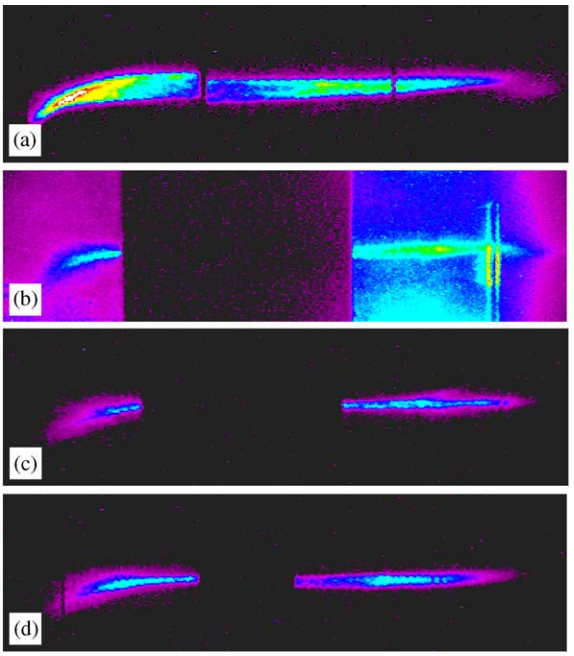

Fig. 2. The chirped electron beam at the high-energy slit monitor: [a] closed slit (500 pC, 2.8% chirp); [b] fully open slit (60% transmission); [c] compressed fraction of the beam (1.5% chirp); and [d] the fraction of a beam generating a single SASE spike (0.8% chirp).

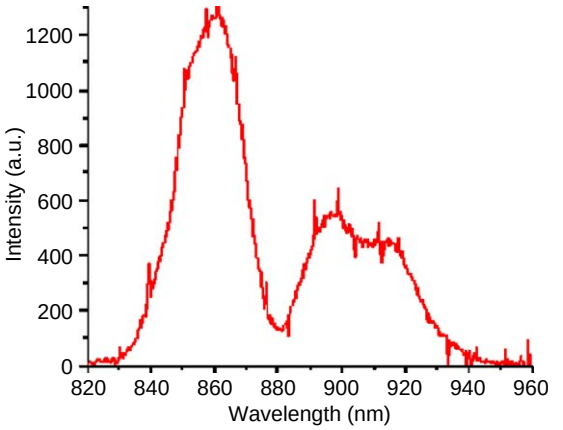

Fig. 3. SASE spectrum width—with the strongly chirped beam—reaches up to 10%.

4. Beam line improvements and outlook for the future

While the studies shown above are still under way to investigate the limits of the chirped beam amplification, there steps have been undertaken to improve the VISA experimental system in the near future. First and foremost, the magnetic chicane has been built and installed into the H-line [10] at the ATF (Fig. 4). Numerical simulations show that using the chicane one can increase the peak current in the electron beam by an order of magnitude without the need to use nonlinear properties of the dispersive section. Furthermore, the second order effects in the dispersive section utilized during the VISA-I and initial period of VISA-II experiments may become parasitic with the introduction of the chicane and would degrade the performance of the system. To avoid these problems, a set of sextupoles is being installed into the dispersive section [11], which according to simulations can linearize the transport even for the strongly chirped beams.

The chicane and sextupoles will be commissioned before the end of 2003. In addition to beam line modifications, the diagnostics at VISA are being upgraded. The longitudinal electron beam diagnostics, including the CTR interferometer, is under development before and after the dispersive section. Also, additional beam profile monitors are being installed in the beam line 3, as well as upgraded SASE optical diagnostics. In addition there are plans for autocorrelation of the SASE light at the undulator exit.

In conclusion, here we report operation of the high gain SASE FEL driven by the strongly chirped electron beam. SASE spectra indicate very large energy spread in the lasing portion of the beam, as well as short pulse duration. In parallel, the ongoing upgrades to VISA beam line will improve in the near future the control over the electron beam longitudinal phase space, as well as transport efficiency, which will enable unambiguous chirped pulse amplification studies throughout the next year.

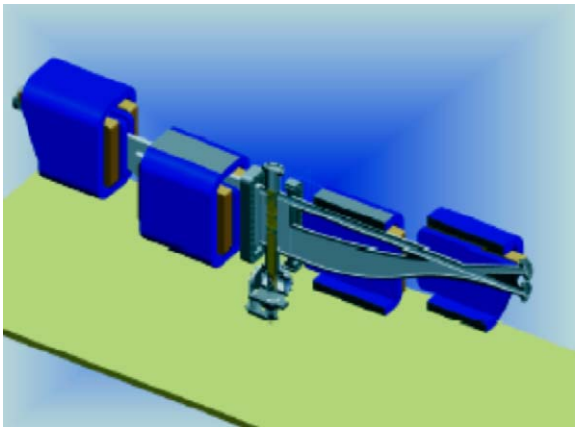

Fig. 4. Rendered drawing of the UCLA/ATF chicane.

Acknowledgements

The authors thank M. Woodle and the ATF staff for technical support, and also BNL Cottage #30 for inspiration. The work is performed under ONR Grant # N00014-02-1-0911.

References

[1] M. Cornacchia, Nucl. Instr. and Meth. A, (2004) these Proceedings.
[2] R. Neutze, et al., Nature 406 (2000) 752.
[3] C. Pellegrini, unpublished technote, 1999.
[4] C. Schroeder, et al., J. Opt. Soc. Am. B 19 (2002) 1782.
[5] S. Krinsky, Z. Huang, Phys. Rev. STAB 6 (2003) 050702.
[6] R. Bonifacio, et al., Phys. Rev. Lett. 73 (1994) 70.
[7] A. Tremaine, et al., Phys. Rev. Lett. 88 (2002) 204801.
[8] A. Murokh, et al., Phys. Rev. E 67 (2003) 066501.
[9] G. Andonian, et al., Proceedings of PAC 2003, Portland, April 2003.
[10] R. Agustsson, UCLA Master Thesis, 2004.
[11] J. England, private communication.